Self-bound clusters of one-dimensional fermionic mixtures

M. C. Gordillo*

Departamento de Sistemas Físicos, Químicos y Naturales, Universidad Pablo de Olavide, Carretera de Utrera Kilmetro 1, E-41013 Sevilla, Spain
and Instituto Carlos I de Física Teórica y Computacional, Universidad de Granada, E-18071 Granada, Spain

(Received 6 July 2023; accepted 18 October 2023; published 13 November 2023)

Diffusion Monte Carlo calculations on the possibility of having self-bound one-dimensional droplets of SU(6) × SU(2) ultracold fermionic mixtures are presented. We found that, even though arrangements with attractive interactions with only two spin types are not self-bound, mixtures with at least three kinds of fermions form stable small drops. However, that stabilization decreases for very tight confinements, where a universal behavior is found for Fermi-Fermi and Fermi-Boson clusters including attractive and repulsive interactions.

DOI: 10.1103/PhysRevResearch.5.043144

I. INTRODUCTION

In a liquid droplet the attractive interaction between particles should be balanced by repulsive forces in order to prevent the collapse of the system [1]. That is as true in a classical setting as when we are dealing with the ultradilute quantum drops [2] observed in Bose-Bose mixtures with either isotropic [3–5] or dipolar interactions [6,7]. In the context of ultradilute cold atoms, which is the one we will be limited to in this work, liquid is customarily understood as a synonym of self-bound, i.e., with a lower (more negative) energy than that of the isolated units that constitute it (see, for instance, Refs. [1–3,8–11]). In particular, it does not imply any particular kind of internal structure different from that of a gas as it does in condensed-matter physics. The study of these self-bound systems started after a suggestion by Petrov [12] (even though there is at least a work [13] on the same topic that predates it), whose theoretical study of binary bosonic arrangements with both attractive and repulsive interactions showed that terms of purely quantum origin prevented the collapse predicted by mean-field descriptions. Examples of those liquid bosonic droplets and their stability limits could be found already in the literature [2,9–11,14–17].

Beyond that frame, we can find works dealing with mixtures of ultracold bosons and fermions [8,18–22], whose stability for repulsively interacting bosons was found to be enhanced in one-dimensional (1D) setups [8]. All those studies use in some form or another mean-field approximations and are limited (except for the homogeneous arrangements in Ref. [22]) to the weakly interacting regime and to clusters in which the number of fermions is much smaller (ranging from an order of magnitude smaller to a single impurity) than the number of bosons. Considering all this, the goal of this work is to go further with boson-boson and boson-fermion mixtures in two ways: first, we explore the possibility of having stable self-bound 1D drops made up exclusively of fermions with no bosons included. In a sense, this is a continuation of previous work on similar systems (see, for instance, Refs. [23–27]), but for a number of fermion species larger than two. Second, since a set of distinguishable fermions can be considered effectively as a set of bosons, we explore the stability limits of small 1D Bose-Fermi droplets in the strong interacting limit, including correlations effects that are out of reach of mean-field approximations. We also establish the minimum droplet composition to have self-bound droplets.

It is well known that a couple of spin-up and spin-down 1D fermions that attract each other via a δ potential will pair to form a "molecule" irrespectively of the strength of their interaction [28]. This means that, in principle, if we have a set of two different kinds of fermions with the same number of atoms each, we will have as many "molecules" as the number of particles of each set. What we do not know is how those molecules interact with each other and how the internal spin composition of the 1D clusters affects the possible phases we may have. To study that, we analyze mixtures of the fermionic isotopes of ytterbium, ^{173}Yb and ^{171}Yb [29–31]. The atoms of the first species can have up to six different spin values [SU(6) symmetry], while the second is a more conventional SU(2) arrangement [30], similar to ^{6}Li. These systems have several advantages: first, those mixtures have already been obtained [31], which means that the conclusions of this work can be experientially checked; second, their masses, m, are close enough to be modeled by a single parameter. This simplifies considerably the picture, since we do not have to take into account the effect of mass imbalance. And last, the strong attraction between the ^{173}Yb and ^{171}Yb atoms produces always molecules belonging to different isotopes, irrespective of the spin composition of the mixture. This means that when we have spin-polarized ^{173}Yb and ^{171}Yb the system is equivalent to a conventional SU(2) system made up of, for instance, ^{6}Li atoms that have only two spin states.

*cgorbar@upo.es

Considering all of the above, we have studied mixtures of ^{173}Yb and ^{171}Yb with different spin compositions in one-dimensional environments. In accordance with previous literature, and given the very low temperatures at which experiments involving ultracold atoms are done, we suppose those systems to be adequately described by the ground state (equivalent to consider $T = 0$) of the strictly 1D Hamiltonian [32,33]:

$$H = \sum_{i=1}^{N_p} \frac{-\hbar^2}{2m}\nabla_i^2 + g_{1D}^{173-171} \sum_{i=1}^{N_{173}} \sum_{j=1}^{N_{171}} \delta\left(x_i^{173} - x_j^{171}\right) + g_{1D}^{173-173} \sum_{b>a}^{6} \sum_{i=1}^{n_{173,a}} \sum_{j=1}^{n_{173,b}} \delta\left(x_{a,i}^{173} - x_{b,j}^{173}\right) + g_{1D}^{171-171} \sum_{b>a}^{2} \sum_{i=1}^{n_{171,a}} \sum_{j=1}^{n_{171,b}} \delta\left(x_{a,i}^{171} - x_{b,j}^{171}\right), \quad (1)$$

Here, N_p is the total number of fermions, and N_{173} and N_{171} are the total number of ^{173}Yb and ^{171}Yb atoms. In this work, we dealt only with balanced clusters, i.e., $N_{173} = N_{171} = N_p/2$. No harmonic potential in the x direction that could spuriously stabilize the drops was imposed. $n_{173,ab}$ and $n_{171,ab}$ are the number of atoms with spins a and b. The second term in Eq. (1) takes into account the interactions in which a member of a pair is a ^{173}Yb atom and the other a ^{171}Yb particle, which do not depend on spin [29], so the positions of the particles, $x_{i,j}$, are labeled by isotope type only. On the other hand, the next two terms deal with ^{173}Yb - ^{173}Yb and ^{173}Yb - ^{171}Yb pairs, so the different spin types a and b have to be included in the position labels. No interactions were considered for fermions of the same species, since those were kept apart by Pauli's exclusion principle.

Since we are interested in self-bound systems, we do not include a longitudinal confinement in the x direction, something usually done by the introduction of a term of the type $1/2m\omega_\parallel^2 x_i^2$. The transverse confinement that produces the 1D setup is included in an effective way in the g_{1D} parameters defined below [34], and it is customarily described by a radial harmonic oscillator with differences between consecutive energy levels given by $\hbar\omega_\perp$. Those levels are not populated beyond the ground state since $\omega_\parallel = 0 \ll \omega_\perp$ [35]. This means that it is more favorable for the particles of the system to accommodate any possible repulsive effective interactions by spreading in the longitudinal direction than to be promoted to the next transverse mode. In addition, when we have more than two spin species the interaction between molecules is attractive (see Results section below), which implies that to promote some of those units to the next transverse mode we have to provide the energy to overcome that attraction.

The values of the g_{1D}'s can be obtained via $g_{1D}^{\alpha,\beta} = -2\hbar^2/ma_{1D}(\alpha,\beta)$, where the 1D scattering lengths, a_{1D}, are defined by [34]

$$a_{1D}(\alpha,\beta) = -\frac{\sigma_\perp^2}{a_{3D}(\alpha,\beta)}\left(1 - A\frac{a_{3D}(\alpha,\beta)}{\sigma_\perp}\right), \quad (2)$$

with $A = 1.0326$. $\sigma_\perp = \sqrt{\hbar/m\omega_\perp}$ is the oscillator length in the transversal direction, depending on the transversal confinement frequency $\omega_\perp$. This implies that the transverse confinement is harmonical and not of any other type, for instance, boxlike. $a_{3D}(\alpha,\beta)$ stands for the three-dimensional set of scattering lengths taken from Ref. [29], i.e., 10.55 nm (^{173}Yb - ^{173}Yb), -0.15 nm (^{171}Yb - ^{171}Yb), and -30.6 nm (^{171}Yb - ^{173}Yb) [29], where the minus signs mean attractive interactions. We considered that the only source of change for a_{1D} comes from variations in the transverse confinement, since modifying the three-dimensional scattering lengths in Yb isotopes is problematic due to their particular electronic structure [30]. This means that the type of interaction between atoms is fixed by the sign of the scattering length in three dimensions: a negative $a_{3D}(\alpha,\beta)$ implies $g_{1D}^{\alpha,\beta} < 0$ (attractive) and vice versa.

II. METHOD

To check if one can have self-bound 1D drops of ^{173}Yb and ^{171}Yb atoms we have to solve the Schrödinger equation derived from the Hamiltonian of Eq. (1) with free boundary conditions. This means that no spurious periodicity and no confining external potential (such as one or several hard walls or an harmonic term) is imposed on the system. Under such conditions, the solutions corresponding to that Hamiltonian in the absence of interaction between atoms are waves with any possible (positive) energy value in a continuous spectrum [28]. To solve the full problem, we used the fixed-node diffusion Monte Carlo method [36], which provides us with an exact solution within some statistical uncertainties, for the ground state ($T = 0$) of a system of interacting fermions when the positions of the nodes of the exact wave function describing the system are known. Fortunately, in strictly 1D systems we can have nodes only when two particles are exactly on top of each other [37]. This information is easily included in the so-called *trial* function, which is the initial approximation to the many-body real wave function the DMC algorithm needs. The use of a Monte Carlo method allows us to go beyond mean-field approximations by introducing correlations between particles, something that can be necessary to describe accurately dilute gas systems (see, for instance, Refs. [12,38], which provide a comparison of mean-field, quantum Monte Carlo, and experiment for one of those systems). When the trial wave function happens to be the real many-body function describing the system, the DMC technique gives us the value of the energy without statistical errors.

Following Refs. [32,33], we used the following as a trial function:

$$\Phi\left(x_1,\ldots,x_{N_p}\right) = \mathcal{A}\left[\phi(r_{11'})\phi(r_{22'})\cdots\phi\left(r_{N_{173},N_{171}}\right)\right] \times \prod_{b>a}^{6}\prod_{i=1}^{n_{173,a}}\prod_{j=1}^{n_{173,b}} \frac{\psi\left(x_{a,i}^{173} - x_{b,j}^{173}\right)}{\left(x_{a,i}^{173} - x_{b,j}^{173}\right)} \times \prod_{b>a}^{2}\prod_{i=1}^{n_{171,a}}\prod_{j=1}^{n_{171,b}} \frac{\psi\left(x_{a,i}^{171} - x_{b,j}^{171}\right)}{\left(x_{a,i}^{171} - x_{b,j}^{171}\right)}, \quad (3)$$

where $\mathcal{A}[\phi(r_{11'})\phi(r_{22'})\cdots\phi(r_{N_{173},N_{171}})]$ is the determinant of a square matrix whose dimension is $N_{173} \times N_{171}$ [39] (for a balanced cluster $N_{173} = N_{171}$) and takes care of the interactions between pairs of particles of different isotopes. $\phi(r_{ij'})$'s are functions that depend on the distance between those particles

$r_{ij'} = |x_i^{173} - x_{j'}^{171}|$ and are chosen as the exact solution of the Schödinger equation corresponding to a pair of nonconfined 1D particles interacting with an attractive δ potential, i.e., [28]

$$\phi\left(\left|x_i^{173} - x_{j'}^{171}\right|\right) = \exp\left[-\frac{\left|g_{1D}^{173,171}\right|}{2}\left|x_i^{173} - x_{j'}^{171}\right|\right]. \quad (4)$$

Since we are dealing with strictly 1D systems, we can take that as an exact solution for the two-body interaction term without the regularization needed in higher dimensions. All this means that we can write any row of $\mathcal{A}[\phi(r_{11'})\phi(r_{22'})\cdots\phi(r_{N_{173},N_{171}})]$ as

$$\exp\left(-\left|g_{1D}^{173,171}\right|r_{i1'}/2\right), \exp\left(-\left|g_{1D}^{173,171}\right|r_{i2'}/2\right), \quad \ldots,$$
$$\exp\left(-\left|g_{1D}^{173,171}\right|r_{i,N_{171'}}/2\right), \quad (5)$$

where i stands for a particular ^{173}Yb and the second index varies to consider all the atoms belonging to the ^{171}Yb isotope, irrespectively of their spin. The use of that structure implies that the trial function is antisymmetric with respect to the interchange of two atoms of the same isotope [39]. It also means that when two same-species atoms are on the same position the trial function is 0, as it should be for a couple of identical fermions.

The above determinant should describe accurately a system in which all ^{173}Yb atoms are spin polarized and the same is true of all the ^{171}Yb ones. However, if we have, for instance, two sets of ^{173}Yb particles with different spins, this is not so. The reason is that the atoms of those two different sets are *distinguishable* particles and not bound by the Pauli exclusion principle. If we still use $\mathcal{A}[\phi(r_{11'})\phi(r_{22'})\cdots\phi(r_{N_{173},N_{171}})]$, we are going to have nodes for positions for which ^{173}Yb atoms of different spins are on top of each other, something that is, in principle, not true.

To correct that, we have to look at how the determinant is built. We can write down two consecutive rows accounting for the interaction of two distinguishable atoms at coordinates x_i and x_j in the ^{173}Yb subset with all the ^{171}Yb particles (at coordinates $x_{1'}, x_{2'}, \ldots, x_{N_{171'}}$) as

$$\begin{vmatrix} \exp\left(-\left|g_{1D}^{173,171}\right|r_{i1'}/2\right) & \cdots & \exp\left(-\left|g_{1D}^{173,171}\right|r_{i,N_{171'}}/2\right) \\ \exp\left(-\left|g_{1D}^{173,171}\right|r_{j1'}/2\right) & \cdots & \exp\left(-\left|g_{1D}^{173,172}\right|r_{j,N_{171'}}/2\right) \end{vmatrix},$$

and when $x_i \to x_j$, we can write

$$\begin{aligned}\phi(r_{ik'}) &= \exp\left(-\left|g_{1D}^{173,171}\right||x_i - x_{k'}|/2\right) \\ &= \exp\left(-\left|g_{1D}^{173,171}\right||x_j + \Delta - x_{k'}|/2\right), \end{aligned} \quad (6)$$

with $\Delta = x_i - x_j \to 0$. Expanding to the first order in Δ, we have

$$\phi(r_{ik'}) = \phi(r_{jk'}) - \left|g_{1D}^{173,171}\right|\frac{\exp\left(-\left|g_{1D}^{173,171}\right|r_{jk'}/2\right)(x_j - x_{k'})\Delta}{2r_{jk'}}. \quad (7)$$

This means that we can write $\mathcal{A}[\phi(r_{11'})\phi(r_{22'})\cdots\phi(r_{N_{173},N_{171}})]$ as a sum of two determinants, the first one with two equal rows (and hence null) and the second one including the correction given by the last term of the right-hand side of Eq. (7). With that in mind, we can see that the origin of the spurious node at $x_i - x_j \to 0$ is the dependence of all the elements of that determinant row on Δ. This can be corrected by dividing those elements by, in this case, $x_i - x_j$. This is completely equivalent to considering a factor $1/(x_i - x_j)$ in the trial function. We can repeat this procedure for any pair of distinguishable atoms in the ^{173}Yb and ^{171}Yb ensembles. This is the origin of the terms $(x_{a,i}^{\alpha} - x_{b,j}^{\alpha})$ in the denominator of Eq. (3) [32,33].

$\psi(x_{a,i}^{\alpha} - x_{b,j}^{\alpha})$ ($\alpha = 173$ and 171) is a Jastrow function that introduces the correlations between pairs of particles of the same isotope belonging to different spin species a and b. Particles of the same isotope with the same spin are assumed to interact via Pauli exclusion only. For the ^{173}Yb - ^{173}Yb pair, we have chosen, following the previous literature for a pair of repulsively interacting particles [40],

$$\psi\left(x_{a,i}^{173} - x_{b,j}^{173}\right) = \begin{cases} \cos\left(k\left[\left|x_{a,i}^{173} - x_{b,j}^{173}\right| - R_m\right]\right) & \left|x_{a,i}^{173} - x_{b,j}^{173}\right| < R_m, \\ 1 & \left|x_{a,i}^{173} - x_{b,j}^{173}\right| \geqslant R_m, \end{cases} \quad (8)$$

where k was obtained by solving

$$k a_{1D}(173, 173)\tan(kR_m) = 1 \quad (9)$$

for each value of $a_{1D}(173, 173)$ deduced from Eq. (2) for a given transverse confinement. $\omega_{\perp}$ was taken in the range $2\pi\times$0–100 kHz, in line with previous experimental values [41]. The value of R_m was the output of a variational calculation. When the pair of particles of the same isotope attract each other, as in the ^{171}Yb - ^{171}Yb case, the Jastrow has the form of Eq. (4) [32,40], but with a different value of the defining constant $g_{1D}^{171,171}$.

DMC being a statistical method, one has to be careful to avoid all possible sources of error. The first one comes from spurious correlations. Those could arise when we perform a single simulation and average the results after every single DMC step. To avoid that, for each Monte Carlo history comprising 2.5×10^5 steps (after thermalization), we used configurations separated by 100 Monte Carlo steps to obtain the averages. This means 2500 values instead of 2.5×10^5. In addition, all the energies and other observables given below are the result of averaging six different Monte Carlo histories and the error bars will correspond to the standard deviations of those six values. This follows closely the procedure of Ref. [32]. The second source of error could come from the election in the number of walkers N_w. Following Refs. [32,42], we performed a study of the convergence of the energy (after decorrelation) as a function of that parameter and found that any number of walkers equal or larger than 1000 produced the same values. For instance, for a cluster

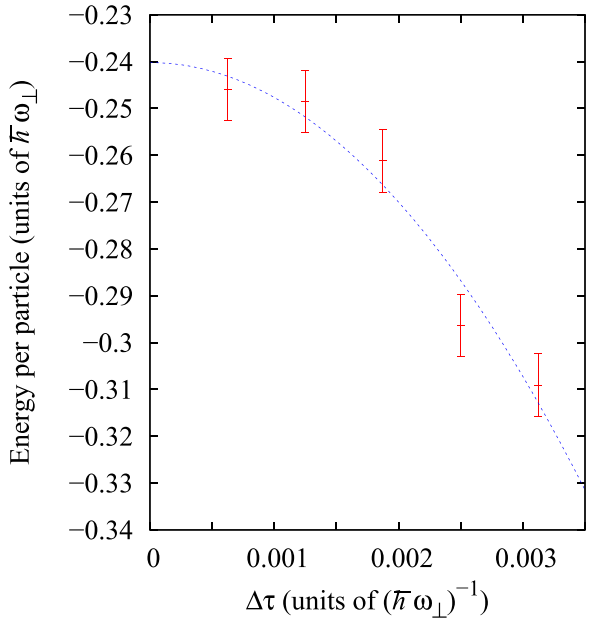

FIG. 1. Dependence of the DMC energy per particle on the DMC time step ($\Delta\tau$) for a cluster with two sets of three ^{173}Yb atoms and a spin-polarized subcluster with six ^{171}Yb particles for $\omega_\perp/(2\pi) =$ 25 kHz. The number of walkers was $N_w = 1000$.

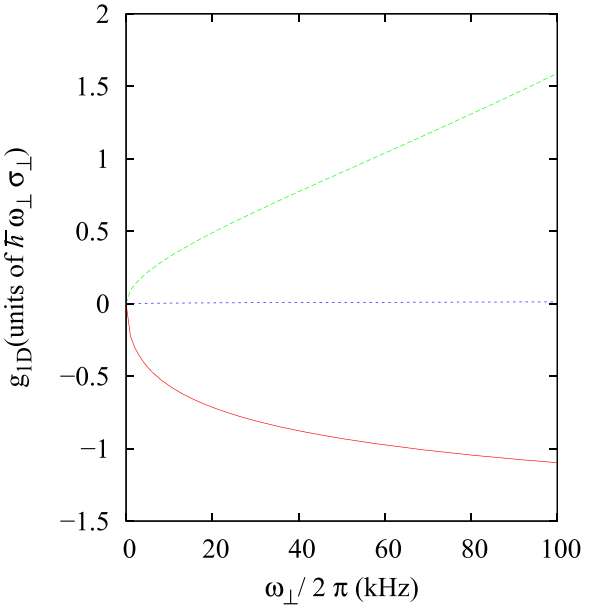

FIG. 2. Dependence of the g_{1D} parameters of Eq. (1) on the transverse confinement $\hbar\omega_\perp$. Full line, $g_{1D}^{173-173}$; dashed line, $g_{173-171}^{1D}$; dotted line, $g_{1D}^{171-171}$.

comprising 12 particles, with two sets of three ^{173}Yb atoms with different spins and six spin-polarized ^{171}Yb atoms, we have that for a time step of $\Delta\tau = 6\times10^{-4}\ (\hbar\omega_\perp)^{-1}$ the energy values per particle for $\omega_\perp/(2\pi) = 25$ kHz (the experimental value of Ref. [41]) were $-0.246 \pm 0.007\ \hbar\omega_\perp$ for $N_w = 1000$, $-0.249 \pm 0.007\ \hbar\omega_\perp$ for $N_w = 1500$, and $-0.248 \pm 0.007\ \hbar\omega_\perp$ for $N_w = 2000$, all within the error bars of each other. This justifies the election of 1000 walkers for all the energy results given below. This is the same number used in Ref. [32] for a similar system.

Another possible source of error is the DMC time step $\Delta\tau$. Figure 1 shows the results of the extrapolation of the energy to the limit $\Delta\tau \to 0$ for the same cluster considered above. In that figure, the dotted line is a least-squares fit to a quadratic form corresponding to the propagator used [43]. The energy per particle, including the error bars derived from the fitting procedure, is $-0.240 \pm 0.005\ \hbar\omega_\perp$, within the error bar of the value obtained for $\Delta\tau = 6\times10^{-4}\ (\hbar\omega_\perp)^{-1}$. From that and after having done similar studies in other clusters, we concluded that an adequate value for the DMC time step was $\Delta\tau = 6\times10^{-4}\ (\hbar\omega_\perp)^{-1}$. We have also tested that this time step was large enough to provide a proper sampling of all the possible particle configurations.

III. RESULTS

To solve the Schrödinger equation derived from the Hamiltonian in Eq. (1), we need to deduce the g_{1D} parameters for the interactions between ytterbium isotopes. This can be done with the help of Eq. (2), which relates the physical magnitudes that define the system (m, $\omega_\perp$, and the different three-dimensional scattering lengths a_{3D}) to the corresponding g_{1D}'s. Of those magnitudes, m and a_{3D} are fixed, but we can change $\omega_\perp$ ($2\pi\times$0–100 kHz) to modify the effective interaction between particles. The results of such variation on the values of the g_{1D}'s are displayed in Fig. 2. There, we can see that the ^{173}Yb - ^{173}Yb interaction is always repulsive, while the ^{173}Yb - ^{171}Yb is always attractive and of the same order of magnitude. At the same time, $g_{1D}^{171,171} \sim 0$ in all the $\omega_\perp$ range. It is also important to stress that we have chosen to consider only interaction parameters compatible with experimental conditions. This means that, for instance, the ratio $g_{1D}^{173,173}/g_{1D}^{173,171}$ cannot be varied arbitrarily, being fixed by Eq. (2). With that in mind, we solved the Schrödinger equation corresponding to the Hamiltonian in Eq. (1) for a set of balanced clusters with different number of total particles, $N_p = 4$, 6, 8, 10, and 12.

We started with arrangements in which all the ^{173}Yb and ^{171}Yb atoms were spin-polarized, i.e., belonged to the same spin species. That system would be similar to a set of paired spin-up and spin-down ^{6}Li atoms. For *all* values of the transverse confinement, the total energy was $-N_pE_b/2$, with E_b being the binding energy between ^{173}Yb - ^{171}Yb pairs with no statistical error. That energy is [28,35]

$$E_b = \frac{\hbar\omega_\perp}{4}\left(\frac{g_{1D}^{173,172}}{\hbar\omega_\perp\sigma_\perp}\right)^2. \tag{10}$$

This means that the particles arranged themselves in pairs formed by atoms of different isotopes with no attraction between them. As indicated above, this implies that the trial function including a single determinant of the type $\mathcal{A}[\phi(r_{11'})\phi(r_{22'})\cdots\phi(r_{N_{173},N_{171}})]$ is the real wave function of the system of pairs. This is similar to what happens in three dimensions but with a subtle difference: for instance, in Ref. [44], the system had periodic boundary conditions, and the total energy, after subtracting the energy corresponding to the binding of the pairs, was positive, not 0 as in our

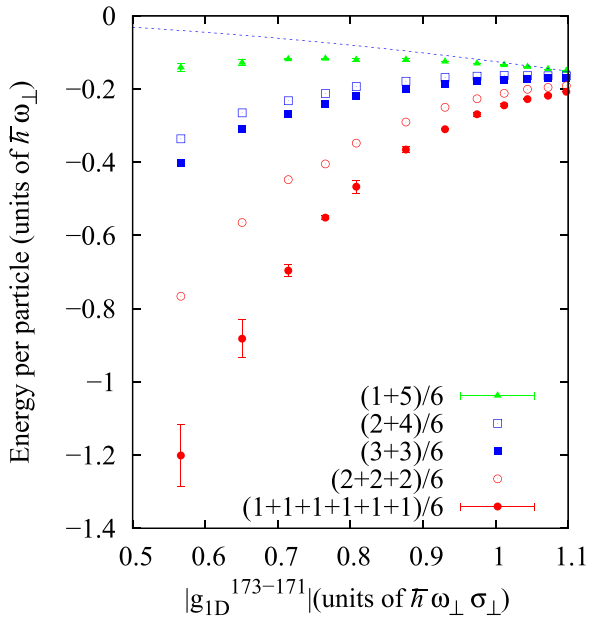

FIG. 3. Energy per particle in units of $\hbar\omega_\perp$ for a set of balanced clusters with the total number of particles N_p equal to 12 as a function of the $|g_{1D}^{173-171}|$ parameter. The clusters are named as $(\sum_{a=1}^{s_{173}} n_{173,a})/(\sum_{b=1}^{s_{171}} n_{171,b})$. The energies of two of the droplets are given with their corresponding error bars. When not shown, those bars are of the same size as the ones displayed for the same values of $|g_{1D}^{173-171}|$. The dotted line corresponds to $E_b/2 = -(g_{1D}^{173-171})^2/8$.

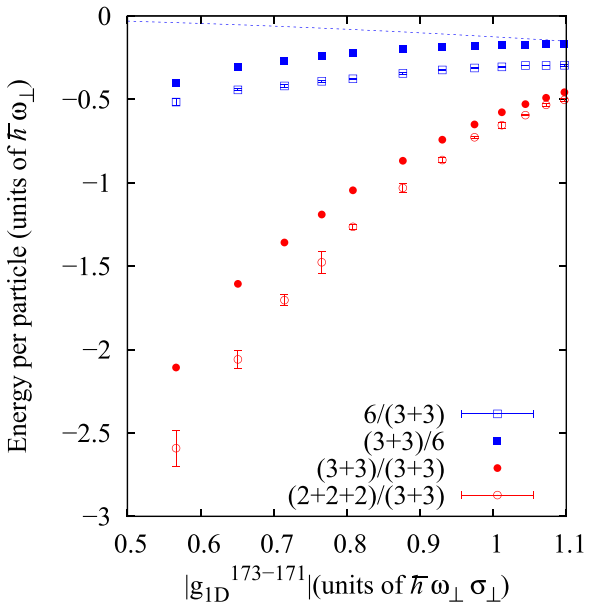

FIG. 4. Same as in the previous figure but for clusters of different compositions. In the $6/(3+3)$ cluster, the error bars are of the same size as the symbols.

free boundary conditions arrangement. Those molecules do not interact with each other due to the avoidance of *both* elements of the pair by fermions of the same species in other pairs brought about by the Pauli exclusion principle. That precludes the formation of self-bound drops, and it should be a common property of any SU(2) balanced system with very short-range (δ or its counterpart in higher dimensions) attractive interactions. Thus, to check if a droplet is stable, we have to verify that the total energy of the cluster is below $-N_pE_b/2$, i.e., more negative than that corresponding to a set of noninteracting paired molecules. This is exactly the same criterion used in ^{3}He drops [45–47].

Figure 3 reflects the change in the previous situation when we have more than one spin species for the ^{173}Yb set of atoms and keep the ^{171}Yb spin polarized. There, we display the energy per particle for balanced clusters with $N_p = 12$ in units of $\hbar\omega_\perp$ as a function of the absolute value of $g_{1D}^{173-171}$ (in units of $\hbar\omega_\perp\sigma_\perp$). Those units are the ones customarily used in the literature and can be translated into experimental physical magnitudes via Eq. (2). From Eq. (10), we can deduce that the energy per particle of a spin-polarized cluster should be $-E_b/2 = -(g_{1D}^{173-171})^2/8$, the value displayed in Fig. 3 as a dotted line. What we see is that for small values of $|g_{1D}^{173-171}|$, corresponding to relatively loose confinements, the energy per particle for any cluster composition becomes appreciably more negative than the one for the case of two spin-polarized isotopes, but that for tighter confinements (larger $|g_{1D}^{173-171}|$'s) it gets progressively closer to that number. The fact that the total energy of the clusters is lower than that corresponding to a set of $N_p/2$ pairs is the signature of a self-bound system, as it can be seen in Ref. [48] for a single light impurity embedded in a 1D system of heavier atoms.

From the analysis of Fig. 3 we can obtain several conclusions. First, we can see that it is enough to flip a single spin in the ^{173}Yb set to obtain a self-bound droplet. This can be deduced from the result for a $(1+5)/6$ cluster, but it is also applicable to an ^{171}Yb flip in a $6/(5+1)$ arrangement, whose energies are not given by simplicity. This stabilization is due to the relaxation of the Pauli-related restrictions, which allows, in the first case, a single ^{171}Yb atom to be close to several ^{173}Yb atoms of different spins. At the same time, those ^{173}Yb atoms can be arbitrarily close together since they belong to different species. The only price to pay will be a repulsive ^{173}Yb - ^{173}Yb interaction (not avoidance as for undistinguishable fermions) that can be counterbalanced by the attraction between atoms of different isotopes. Obviously, the effects of this relaxation increase with the number of different spin species, making the arrangements progressively more stable. Thus, the system with the lowest energy per particle comprises six *distinguishable* ^{173}Yb and six spin-polarized ^{171}Yb, and it is equivalent to a Fermi-Bose arrangement with a Fermi/Bose ratio of 1:1. This system is stable for all the $g_{1D}^{173-171}$ (and hence $\omega_\perp$) values considered in this work. The mean-field approximation used in Ref. [8] would preclude the stability of those clusters for the lowest values of $g_{1D}^{173-171}$.

The conclusions of the previous paragraphs are fully supported by the study of similar or smaller clusters of different compositions. For instance, in Fig. 4 we can see the effect that the consideration of different numbers of species have for $N_p = 12$. The $(3+3)/6$ case is repeated from the previous figure to serve as a comparison. The overall behavior of the droplets is similar to that shown in Fig. 3: there is a sizable stabilization for relatively loose transverse confinement, and stabilization is reduced for very thin tubes. We can see also that the larger the number of spin species is, the lower the

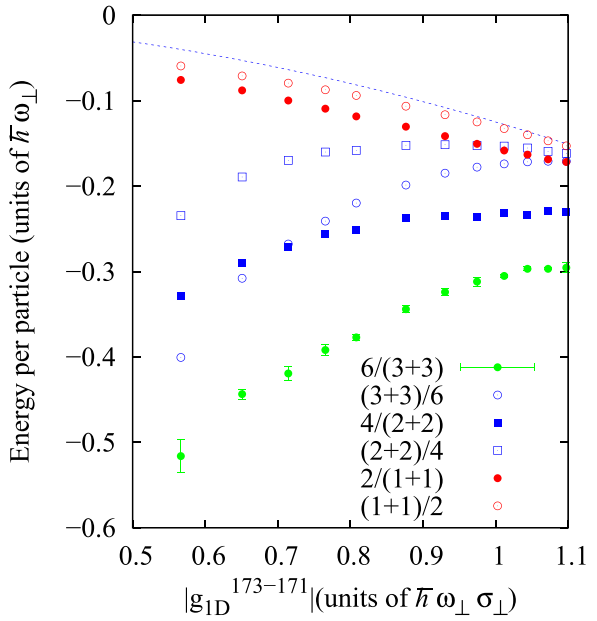

FIG. 5. Energy comparisons between clusters of similar compositions but different total numbers of particles.

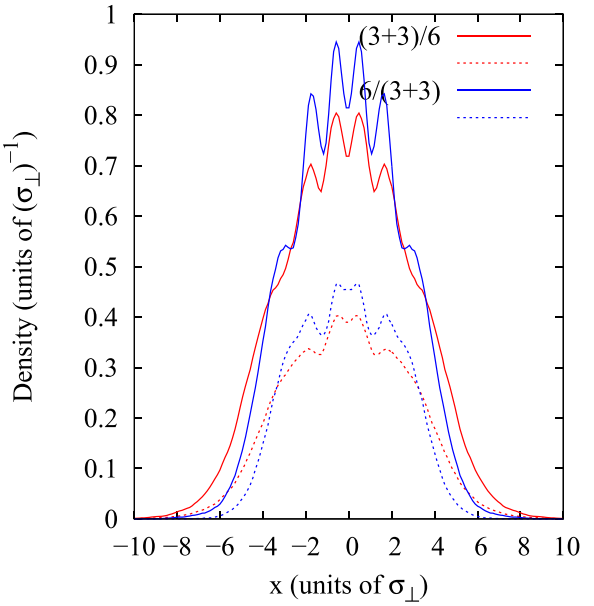

FIG. 6. Density profiles of the $(3+3)/6$ and $6/(3+3)$ clusters for $\omega_\perp = 2\pi\times 25$ kHz. Solid lines, spin-polarized isotopes; dotted lines, other species. The density profiles are normalized to the number of particles, i.e., six or three, respectively. The center of the cluster corresponds to the position of its center of mass.

energy per atom is. In addition, clusters with the same number of species but in which we kept the ^{173}Yb atoms spin polarized are more stable than the ones with spin-polarized ^{171}Yb's. This is due to the weak attraction between ^{171}Yb - ^{171}Yb pairs that kicks in when the Pauli restrictions are relaxed. A similar set of rules can be applied to understand the clusters displayed in Fig. 5. The only additional information is the increasing of the stabilization of the cluster with size. There, we can see that even clusters with a very small number of particles are stable. This justifies us in the use of clusters with $N_p = 12$ particles, since one would expect further increases in stabilization with size.

That stabilization does not imply the collapse of the clusters. In Fig. 6 we can see the density profiles (number of particles per unit length) corresponding to the $(3+3)/6$ and $6/(3+3)$ droplets. Those were calculated from DMC configurations and could be appreciably different from those obtained by using a mean-field method [38]. To avoid the bias introduced in observables other than the energy in the DMC algorithm, a forward-walking technique was used [49]. Since free boundary conditions were used, the particles were able to wander freely in 1D space. To avoid that effect, we calculated the density profiles taking as the origin of coordinates the center of mass of the cluster. The signature of a stable drop is then a finite width of those profiles, a width that was checked to stay constant throughout each Monte Carlo simulation. This situation is different than that for noninteracting spin-polarized clusters of ^{173}Yb and ^{171}Yb, in which those profiles become progressively wider along the Monte Carlo run. According to that prescription, all the clusters with energies smaller than those corresponding to a set of independent molecules have constant width, as can be been in Figs. 6–8. The form of all the profiles, with their maxima at the center of the cluster, implies that such small clusters are not made up of smaller subunits close together. In Fig. 6 the solid lines correspond to the spin-polarized isotope: ^{171}Yb in the first case, and ^{173}Yb in the second. The profiles are normalized to the number of particles in that part of the arrangement, i.e., six. On the other hand, the dotted lines are the averages for the $(3+3)$ part of those systems, and their areas are as half

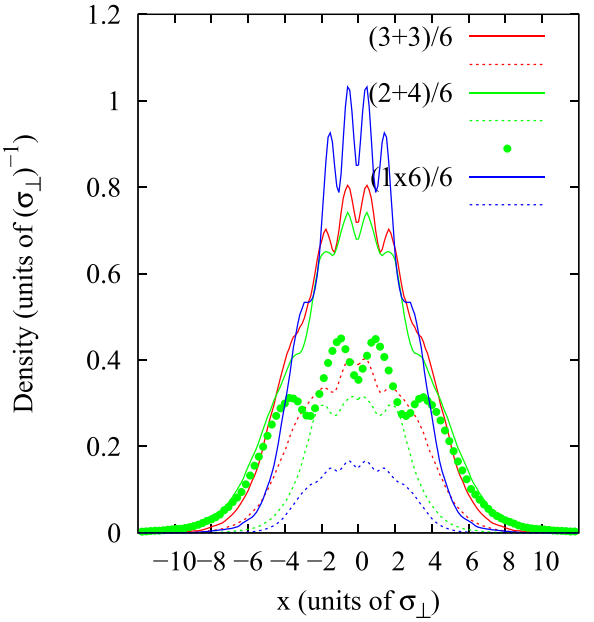

FIG. 7. Same as the previous figure but for clusters of different compositions. Solid lines, spin-polarized ytterbium; dotted lines, minority (or averages of equally distributed) ^{173}Yb atoms; solid circles, majority component in the $(2+4)/6$ clusters. All the densities are normalized to their respective number of atoms. $(1\times 6)/6$ is short for $(1+1+1+1+1+1)/6$. Error bars are of the size of the symbols and not displayed by simplicity.

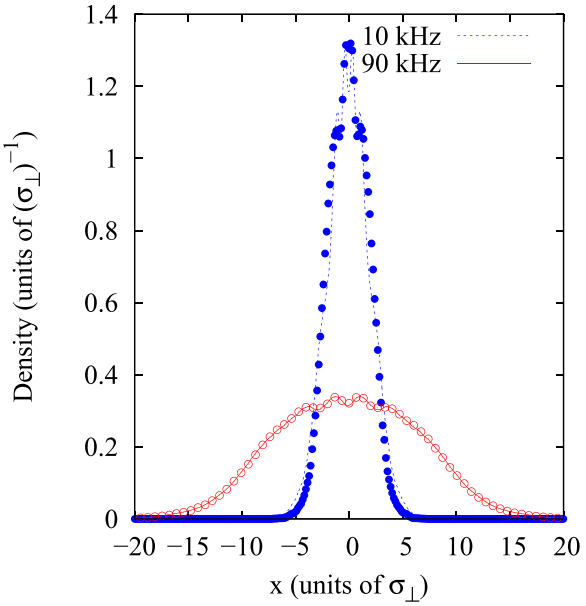

FIG. 8. Density profiles for $(3+3)/6$ clusters for two different values of the transverse confinement: $\omega_\perp = 2\pi \times 10$ kHz (dotted lines and solid spheres) and $2\pi \times 90$ kHz (solid lines and open circles). Lines correspond to the ^{171}Yb isotope and symbols to the ^{173}Yb one. In opposition to the case of Fig. 6 we represented the total density of the last type of atoms, normalizing the profile to six.

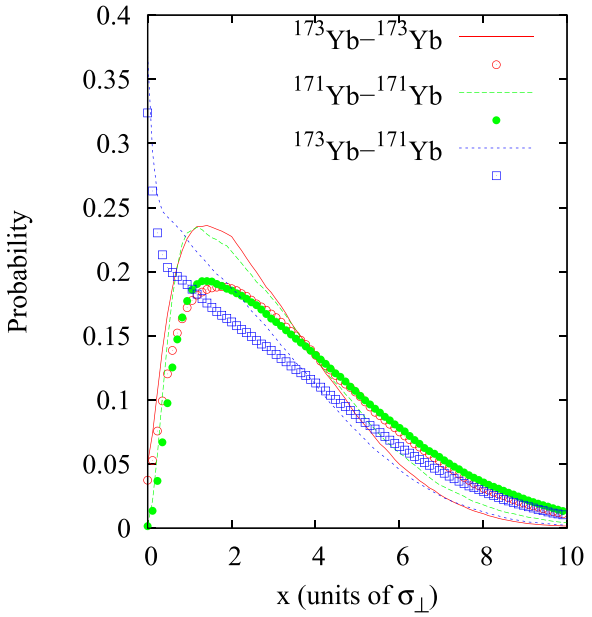

FIG. 9. Probability of finding another particle at a distance x from the first one for $(1+1+1+1+1+1)/6$ (lines) and $(3+3)/6$ (symbols) clusters. The profiles are normalized to one, including the tails beyond $x = 10\sigma_\perp$, not shown for simplicity.

as much as those of their polarized counterparts. The value of the transverse frequency was fixed to $2\pi \times 25$ kHz, the same as the one in the experimental work of Ref. [41] for a set of ^{173}Yb atoms. What we observe is that the width of the clusters is basically the same, but a little bit thinner in the $6/(3+3)$ case, due to the attraction of the ^{171}Yb - ^{171}Yb pairs with different spins, but in any case different from 0. The same can be said of the arrangements displayed in Fig. 7. In this last case, the differences can be ascribed to the different number of spin species of the ^{173}Yb isotope. In all cases we have stable self-bound finite-size drops.

We can also see the influence of the transverse confinement in the shape of the density profiles. In Fig. 8 we can see what happens to the $(3+3)/6$ profile when squeezed in that direction. We have chosen this particular arrangement because, as can be seen in Fig. 5, the energy per particle is noticeably below $-0.5E_b$ for all the values of $|g_{1D}^{173,171}|$ considered. At the same time, the variations in the shape of the profiles are fairly representative of what we can find in other cases. In that figure, we represented both the ^{171}Yb profiles (lines) and the sum of the ^{173}Yb ones (symbols); i.e., this last profile is normalized to six instead of the three in Figs. 6 and 7. What we observe is that, while at low confinements, the total ^{173}Yb and ^{171}Yb distributions are different; at $\omega_\perp = 2\pi \times 90$ kHz, both of them are basically identical. This can be the product of an increase in the repulsion among the atoms of the SU(6) isotope, which makes the system more similar to a set of balanced ^{6}Li atoms. In any case, the similarity is not complete, since there is an energy excess that stabilizes the ytterbium clusters and will not do the same for a set of ^{6}Li atoms. This figure, together with the previous ones, can be used to attest the one dimensionality of the system: the minimum spread on the longitudinal direction corresponds to $\sim 10\ \sigma_\perp$ for $\omega_\perp/(2\pi) = 10$ kHz, with typical values of 15–20 $\sigma_\perp$ at the experimental frequency of $\omega_\perp/(2\pi) = 25$ kHz (see Figs. 6 and 7) and going up to $\sim 40\ \sigma_\perp$ at $\omega_\perp/(2\pi) = 90$ kHz. Those are larger that the value corresponding to the transverse width, by definition, $\sim\sigma_\perp$.

Last, in Fig. 9, we show the probability of finding another particle at a distance x of a given one. This gives us information about the correlations between pairs. Those probabilities were calculated for $(1+1+1+1+1+1)/6$ (lines) and $(3+3)/6$ (symbols) clusters for a transverse confinement of $2\pi \times 25$ kHz. Other arrangements are qualitatively similar and not shown for simplicity. The main features of this observable are covered by representing the probabilities corresponding to all the possible isotope pairs; i.e., all atoms of the same isotope are lumped together. Since in both clusters the ^{171}Yb is spin polarized, the 0 value of that function for a ^{171}Yb - ^{171}Yb pair for $x \to 0$ is simply a consequence of Pauli's exclusion principle. On the other hand, since at least part of the ^{173}Yb atoms belong to different spin species, in that limit the probability of having a ^{173}Yb - ^{173}Yb pair is different from 0. The position of the maxima in both ^{173}Yb - ^{173}Yb and ^{171}Yb - ^{171}Yb functions, roughly similar to each other, reflect the typical distance between different molecules. The existence of those molecules can be deduced from the maxima in the ^{173}Yb - ^{171}Yb probability function for $x \to 0$.

IV. CONCLUSIONS

In this work, we have studied the possibility of the existence of one-dimensional self-bound mixtures of ytterbium fermionic isotopes. To be realistic, experimentally derived parameters were used to describe the interactions

between different species. Since the goal of this work was to establish the possibility of having self-bound clusters and the energy per particle was found to decrease when increasing the number of particles, we stop at $N_p = 12$, since our results indicate that we can expect the trend to continue for larger N_p's. In particular, the study of convergence (if any) to the thermodynamic limit ($N_p \to \infty$) is out of the scope of this work. The criterion to label a cluster as self-bound was to check if its total energy was lower than that corresponding to a set of $N_p/2$ pairs. This implies that the atoms tend to stay together due to that energy decrease and not because of the confinement imposed by an external harmonic potential. This means that the results presented in this work are related, but are not directly comparable to those of Ref. [32], in which that external constraint was imposed.

Several interesting conclusions can be afforded by the analysis of the data above. First, the existence of self-bound 1D droplets made up of two spin-polarized sets of the same number of fermionic atoms with attractive δ interactions is not possible. This is because they form molecules that exclude other pairs in the vicinity due to the double effect of the Pauli exclusion principle between atoms of the same species in different molecules. Even though this is similar to what happens in three-dimensional SU(2) systems with short-range interactions under periodic boundary conditions [44], this effect has not been previously described as such. Second, to flip the spin of a single atom is enough to produce a stable drop. This can be seen with the help of Figs. 3 and 5, which allow one to see that the $(1 + 5)/6$, $2/(1 + 1)$, and $(1 + 1)/2$ clusters are stable. In addition, we have verified that the $6/(5 + 1)$, $4/(3 + 1)$, and $(3 + 1)/4$ clusters are also self-bound and have compact density profiles. Moreover, a close inspection of Figs. 3–5 indicates that any cluster with at least three fermionic species is stable, providing that at least one of the δ interactions between species is attractive. This is a general conclusion that could be experimentally tested.

The third relevant finding of this work has to do with the behavior of the clusters at very tight confinements, i.e., for large values of $|g_{1D}^{173,171}|$ and $g_{1D}^{173,173}$ (see Fig. 1). With the help of Figs. 3–5 we can see that, the tighter the confinement is, the closer the value of the energies per particle to $-E_b/2$ for $(\sum_{a=1}^{s_{173}} n_{173,a})/(N_p/2)$ arrangements is. This means clusters with several spin values for ^{173}Yb and spin polarized in their ^{171}Yb part. This suggests that the $\omega_\perp \to \infty$ energy limit for those clusters is universal and equal to $-E_b N_p/2$. Since a set of $N_p/2$ distinguishable fermions is akin in this context to a set of bosons, that limit would also apply to a 1D Fermi-Boson mixture in which the boson-boson interaction is repulsive. This is corroborated by the behavior of the $(1 + 1 + 1 + 1 + 1 + 1)/6$ and $(1 + 1)/2$ arrangements, displayed in Figs. 3 and 5. In a sense, this is equivalent to the Tonks-Girardeau limit for 1D repulsively interacting single fermions [50], but for pairs of molecules. In that limit, there is no difference between the energies of a set of fermions or bosons for harmonically confined systems. As in the Tonks-Girardeau gas, for very tight confinements we are in the strong interaction limit, something that cannot be dealt with the mean-field approximations used for Fermi-Bose gases in the previous literature [8]. However, the situation is slightly different for $(N_p/2)/(\sum_{a=1}^{s_{171}} n_{171,a})$ clusters, in which fermions with different spins attract each other, even slightly. Then, even though there is still an energy limit for very tight confinement, that limit is lower than that corresponding to $-E_b/2$ per particle (see Fig. 5), as a result of the residual attraction between molecules.

As to the possibility of producing this kind of cluster, we can say that, as indicated above, mixtures of those isotopes have already been obtained [31,51], albeit for larger systems. On the other hand, it is possible to produce very small fermionic drops [52], even in 1D environments [53]. This implies that, *a priori*, the kind of drops considered here can be experimentally produced. Since our results do not preclude the existence of larger self-bound systems with the same compositions, to check that possibility could be worth pursuing. Those clusters could be similar in size and stability to those of Bose-Bose mixtures [3].

Summarizing, this study opens the door to consider new behaviors for attractively interacting fermionic mixtures beyond binary compositions in both 1D and higher dimensions. Those studies need not be limited to mixtures of Yb isotopes, but could be extended to systems made up of atoms with different masses providing we know all the experimentally relevant parameters (m's, scattering lengths, and transverse confinements).

ACKNOWLEDGMENTS

We acknowledge financial support from the Ministerio de Ciencia e Innovación MCIN/AEI/10.13039/501100011033 (Spain) under Grant No. PID2020-113565GB-C22 and from the Junta de Andalucía group PAIDI-205. We also acknowledge the use of the C3UPO computer facilities at the Universidad Pablo de Olavide.

[1] I. Ferrier-Barbut and T. Pfau, Quantum liquids get thin, Science **359**, 274 (2018).

[2] Z. Luo, W. Pang, B. Liu, Y. Y. Li, and B. A. Malomed, A new form of liquid matter: Quantum droplets, Front. Phys. **16**, 32201 (2021).

[3] C. Cabrera, L. Tanzi, J. Sanz, B. Naylor, P. Thomas, P. Cheney, and L. Taurell, Quantum liquid droplets in a mixture of Bose-Einstein condensates, Science **359**, 301 (2018).

[4] P. Cheiney, C. R. Cabrera, J. Sanz, B. Naylor, L. Tanzi, and L. Tarruell, Bright soliton to quantum droplet transition in a mixture of Bose-Einstein condensates, Phys. Rev. Lett. **120**, 135301 (2018).

[5] G. Semeghini, G. Ferioli, L. Masi, C. Mazzinghi, L. Wolswijk, F. Minardi, M. Modugno, G. Modugno, M. Inguscio, and M. Fattori, Self-bound quantum droplets of atomic mixtures in free space, Phys. Rev. Lett. **120**, 235301 (2018).

[6] I. Ferrier-Barbut, H. Kadau, M. Schmitt, M. Wenzel, and T. Pfau, Observation of quantum droplets in a strongly dipolar Bose gas, Phys. Rev. Lett. **116**, 215301 (2016).

[7] D. Edler, C. Mishra, F. Wächtler, R. Nath, S. Sinha, and L. Santos, Quantum fluctuations in quasi-one-dimensional dipolar Bose-Einstein condensates, Phys. Rev. Lett. **119**, 050403 (2017).

[8] D. Rakshit, T. Karpiuk, P. Zin, M. Brewczyk, M. Lewenstein, and M. Gajda, Self-bound Bose–Fermi liquids in lower dimensions, New J. Phys. **21**, 073027 (2019).

[9] D. S. Petrov and G. E. Astrakharchik, Ultradilute low-dimensional liquids, Phys. Rev. Lett. **117**, 100401 (2016).

[10] L. Parisi, G. E. Astrakharchik, and S. Giorgini, Liquid state of one-dimensional Bose mixtures: A quantum Monte Carlo study, Phys. Rev. Lett. **122**, 105302 (2019).

[11] G. De Rosi, G. E. Astrakharchik, and P. Massignan, Thermal instability, evaporation, and thermodynamics of one-dimensional liquids in weakly interacting Bose-Bose mixtures, Phys. Rev. A **103**, 043316 (2021).

[12] D. S. Petrov, Quantum mechanical stabilization of a collapsing Bose-Bose mixture, Phys. Rev. Lett. **115**, 155302 (2015).

[13] A. Bulgac, Dilute quantum droplets, Phys. Rev. Lett. **89**, 050402 (2002).

[14] F. Böttcher, J. N. Schmidt, J. Hertkorn, K. S. H. Ng, S. D. Graham, M. Guo, T. Langen, and T. Pfau, New states of matter with fine-tuned interactions: Quantum droplets and dipolar supersolids, Rep. Prog. Phys. **84**, 012403 (2021).

[15] H. Hu, J. Wang, and X.-J. Liu, Microscopic pairing theory of a binary Bose mixture with interspecies attractions: Bosonic BEC-BCS crossover and ultradilute low-dimensional quantum droplets, Phys. Rev. A **102**, 043301 (2020).

[16] I. Morera, G. E. Astrakharchik, A. Polls, and B. Juliá-Díaz, Quantum droplets of bosonic mixtures in a one-dimensional optical lattice, Phys. Rev. Res. **2**, 022008(R) (2020).

[17] S. P. G. Spada and S. Giogini, Attractive solution of binary Bose mixtures: Lquid-vapor coexistence and critical point, Phys. Rev. Lett. **131**, 173404 (2023).

[18] L. Salasnich, S. K. Adhikari, and F. Toigo, Self-bound droplet of Bose and Fermi atoms in one dimension: Collective properties in mean-field and Tonks-Girardeau regimes, Phys. Rev. A **75**, 023616 (2007).

[19] S. K. Adhikari and L. Salasnich, One-dimensional superfluid Bose-Fermi mixture: Mixing, demixing, and bright solitons, Phys. Rev. A **76**, 023612 (2007).

[20] M. Tylutki, A. Recati, F. Dalfovo, and S. Stringari, Dark–bright solitons in a superfluid Bose–Fermi mixture, New J. Phys. **18**, 053014 (2016).

[21] D. Rakshit, T. Karpiuk, M. Brewczyk, and M. Gajda, Quantum Bose-Fermi droplets, SciPost Phys. **6**, 079 (2019).

[22] J. C. Peacock, A. Ljepoja, and C. J. Bolech, Quantum coherent states of interacting Bose-Fermi mixtures in one dimension, Phys. Rev. Res. **4**, L022034 (2022).

[23] A. Volosniev, D. V. Fedorov, A. S. Jensen, M. Valiente, and N. T. Zinner, Strongly interacting confined quantum systems in one dimension, Nat. Commun. **5**, 5300 (2014).

[24] P. O. Bugnion and G. J. Conduit, Ferromagnetic spin correlations in a few-fermion system, Phys. Rev. A **87**, 060502(R) (2013).

[25] N. Matveeva and G. Astrakharchik, One-dimensional multicomponent Fermi gas in a trap: Quantum Monte Carlo study, New J. Phys. **18**, 065009 (2016).

[26] D. Pecak, M. Gajda, and T. Sowinski, Two-flavour mixture of a few fermions of different mass in a one-dimensional harmonic trap, New J. Phys. **18**, 013030 (2016).

[27] S. Pilati, L. Barbiero, R. Fazio, and L. Dell'Anna, One-dimensional repulsive Fermi gas in a tunable periodic potential, Phys. Rev. A **96**, 021601(R) (2017).

[28] D. Griffiths, *Introduction to Quantum Mechanics*, 2nd ed. (Pearson Prentice Hall, Upper Saddle River NJ, 2005).

[29] M. Kitagawa, K. Enomoto, K. Kasa, Y. Takahashi, R. Ciuryło, P. Naidon, and P. S. Julienne, Two-color photoassociation spectroscopy of ytterbium atoms and the precise determinations of *s*-wave scattering lengths, Phys. Rev. A **77**, 012719 (2008).

[30] M. Cazalilla and A. Rey, Ultracold Fermi gases with emergent SU(N) symmetry, Rep. Prog. Phys. **77**, 124401 (2014).

[31] S. Taie, Y. Takasu, S. Sugawa, R. Yamazaki, T. Tsujimoto, R. Murakami, and Y. Takahashi, Realization of a SU(2) × SU(6) system of fermions in a cold atomic gas, Phys. Rev. Lett. **105**, 190401 (2010).

[32] M. C. Gordillo, Pairing in SU(6)×SU(2) one-dimensional fermionic clusters, Phys. Rev. A **102**, 023335 (2020).

[33] M. Gordillo, Metal and insulator states of SU(6)×SU(2) clusters of fermions in one-dimensional optical lattices, New J. Phys. **23**, 063034 (2021).

[34] M. Olshanii, Atomic scattering in the presence of an external confinement and a gas of impenetrable bosons, Phys. Rev. Lett. **81**, 938 (1998).

[35] M. Casula, D. M. Ceperley, and E. J. Mueller, Quantum Monte Carlo study of one-dimensional trapped fermions with attractive contact interactions, Phys. Rev. A **78**, 033607 (2008).

[36] B. Hammond, W. A. Lester, and P. Reynolds, *Monte Carlo Methods in Ab Initio Quantum Chemistry* (Wold Scientific, Singapore, 1994).

[37] D. Ceperley, Fermion nodes, J. Stat. Phys. **63**, 1237 (1991).

[38] F. Böttcher, M. Wenzel, J.-N. Schmidt, M. Guo, T. Langen, I. Ferrier-Barbut, T. Pfau, R. Bombín, J. Sánchez-Baena, J. Boronat, and F. Mazzanti, Dilute dipolar quantum droplets beyond the extended Gross-Pitaevskii equation, Phys. Rev. Res. **1**, 033088 (2019).

[39] J. Carlson, S.-Y. Chang, V. R. Pandharipande, and K. E. Schmidt, Superfluid Fermi gases with large scattering length, Phys. Rev. Lett. **91**, 050401 (2003).

[40] G. E. Astrakharchik, Quantum Monte Carlo study of ultracold gases, Ph.D. thesis (Universitá degli Studi Trento, 2004).

[41] G. Pagano, M. Mancini, G. Cappellini, P. Lombardi, F. Schäfer, H. Hu, X. J. Liu, J. Catani, C. Sias, M. Inguscio, and L. Fallani, A one-dimensional liquid of fermions with tunable spin, Nat. Phys. **10**, 198 (2014).

[42] M. Boninsegni and S. Moroni, Population size bias in diffusion Monte Carlo, Phys. Rev. E **86**, 056712 (2012).

[43] J. Boronat and J. Casulleras, Monte Carlo analysis of an interatomic potential for He, Phys. Rev. B **49**, 8920 (1994).

[44] G. E. Astrakharchik, J. Boronat, J. Casulleras, and S. Giorgini, Equation of state of a Fermi gas in the BEC-BCS crossover: A quantum Monte Carlo study, Phys. Rev. Lett. **93**, 200404 (2004).

[45] V. R. Pandharipande, S. C. Pieper, and R. B. Wiringa, Variational Monte Carlo calculations of ground states of liquid ^{4}He and ^{3}He drops, Phys. Rev. B **34**, 4571 (1986).

[46] R. Guardiola and J. Navarro, Variational study of ^{3}He droplets, Phys. Rev. Lett. **84**, 1144 (2000).

[47] E. Sola, J. Casulleras, and J. Boronat, Ground-state energy and stability limit of ^{3}He droplets, Phys. Rev. B **73**, 092515 (2006).

[48] A. Tononi, J. Givois, and D. S. Petrov, Binding of heavy fermions by a single light atom in one dimension, Phys. Rev. A **106**, L011302 (2022).

[49] J. Casulleras and J. Boronat, Unbiased estimators in quantum Monte Carlo methods: Application to liquid ^{4}He, Phys. Rev. B **52**, 3654 (1995).

[50] M. D. Girardeau, Two super-Tonks-Girardeau states of a trapped one-dimensional spinor Fermi gas, Phys. Rev. A **82**, 011607(R) (2010).

[51] B. Abeln, K. Sponselee, M. Diem, N. Pintul, K. Sengstock, and C. Becker, Interorbital interactions in an SU(2) $\bigotimes$ SU(6)-symmetric Fermi-Fermi mixture, Phys. Rev. A **103**, 033315 (2021).

[52] M. Holten, R. Klemt, K. Subramanian, J. Bjerlin, S. M. Reimann, G. M. Bruun, P. M. Preiss, L. Bayha, and S. Jochim, Observing the emergence of a quantum phase transition shell by shell, Nature (London) **587**, 583 (2020).

[53] F. Serwane, G. Zürn, T. Lompe, T. B. Ottenstein, A. N. Wenz, and S. Jochim, Deterministic preparation of a tunable few-fermion system, Science **332**, 336 (2011).